

# Chapter 3

## On the Theories of Plates Based on the Cosserat Approach

Holm Altenbach and Victor A. Eremeyev

**Abstract** The classical isotropic linear elastic material behavior is presented by two material parameters, e.g., the Young's modulus and the Poisson's ratio, while the Cosserat continuum is given by six material parameters. The latter continuum model can be the starting point for the deduction of the governing equations of the Cosserat plate theory via a through-the-thickness integration. In contrast, the basic equations of the Cosserat plate theory can be established applying the direct approach. It can be shown that both systems of equations are similar in the main terms. The assumed identity of both systems results in consistent stiffness parameters identification for the two-dimensional theory based on the direct approach and, in addition, in some constraints. Using the experimental results of Lakes, one can show in which cases the additional material properties coming from the three-dimensional Cosserat material model have a significant influence on the stiffness parameters.

### 3.1 Introduction

The continuum model of the Cosserat brothers [5] is founded on the *a priori* introduction of the independence of both the translations and rotations. From this it follows that one symmetric stress tensor is not enough to represent the response of the continuum on the external loadings. The base of such a new continuum model generalizing the Cauchy's model was known since Euler because he introduced two

---

H. Altenbach (✉)

Martin-Luther-Universität Halle-Wittenberg, 06099 Halle (Saale), Germany

e-mail: [holm.altenbach@iw.uni-halle.de](mailto:holm.altenbach@iw.uni-halle.de)

V.A. Eremeyev

South Scientific Center of RASci & South Federal University, Milchakova St. 8a,

344090 Rostov on Don, Russia

e-mail: [eremeyev.victor@gmail.com](mailto:eremeyev.victor@gmail.com)

G.A. Maugin, A.V. Metrikine (eds.), *Mechanics of Generalized Continua*,

Advances in Mechanics and Mathematics 21,

DOI 10.1007/978-1-4419-5695-8\_3, © Springer Science+Business Media, LLC 2010

independent laws of motion: the balance of momentum and the balance of moment of momentum (see [18] among others).

Applications of the Cosserat continuum could not be established for a long time. Only in the 1950s, the Cosserat continuum was recognized as a starting point for various constructions of generalized continuum models. Let us note that some of them are presented for the three-dimensional case to describe complex behavior of solids and fluids. Let us mention here only the pioneering works summarized in the proceedings [11]. In addition, the Cosserat approach was used in establishing less than three-dimensional continuum theories to model shells, plates and rods.

Below we limit our discussion to the plate theory. Any set of governing equations for plates can be deduced using the conventional three-dimensional continuum equations together with the some engineering hypotheses or mathematical techniques. Finally, the manipulated equations are integrated over the thickness. Another possibility is the *a priori* introduction of the two-dimensional field equations for a so-called deformable surface. The latter is an elegant and a more natural way to formulate the plate equations, but the identification of the effective properties is a non-trivial problem. Let us note only some fundamental publications presenting the basic items of the direct approach [9, 16, 17, 8], and the reviews of the Cosserat approach in the shell and plate theories [1, 3].

Here we firstly present two sets of plate equations of the Cosserat type. The first set is introduced by the direct approach, while the second is based on the three-dimensional equations of the Cosserat continuum and a through-the-thickness integration. Secondly, both sets will be compared and analyzed. This way one gets the equivalent terms in both sets showing which terms in the equations introduced by the direct approach correspond to which terms in the integrated three-dimensional equations. As in any dimension-reduction problem, some constraints can be obtained. Last but not least, using the experimental data of Lakes [12, 13] for an open-cell and a closed-cell foam, the influence of the additional material parameters is discussed. It can be shown that in some cases the classical continuum model does not allow the description of the material behavior with a sufficient accuracy, and so a generalized continuum model must be applied.

### 3.2 A Priori Two-Dimensional Governing Equations

Let us introduce the basic equations for micropolar plates based on the direct approach. We consider a deformable plane surface, see Fig. 3.1. Each material point of this surface is an infinitesimal rigid body with 3 translational and 3 rotational degrees of freedom. The balances of momentum and moment of momentum are formulated as follows

$$\begin{aligned} \mathbf{F}_s^* &\equiv \int_{\mathcal{M}_*} \mathbf{q} \, dA + \int_{\mathcal{L}_*} \mathbf{t}_s \, ds = \mathbf{0}, \\ \mathbf{M}_s^* &\equiv \int_{\mathcal{M}_*} (\mathbf{x} \times \mathbf{q} + \mathbf{c}) \, dA + \int_{\mathcal{L}_*} (\mathbf{x} \times \mathbf{t}_s + \mathbf{m}_s) \, ds = \mathbf{0}, \end{aligned} \quad (3.1)$$



**Fig. 3.1** Deformable plane surface

where  $\mathbf{q}$  and  $\mathbf{c}$  are the vectors of surface loads (forces and moments),  $\mathbf{x}$  is the position vector of the plane surface  $\mathcal{M}$ ,  $\times$  denotes the cross-product,  $\mathbf{t}_s$  and  $\mathbf{m}_s$  are the surface analogues of the stress vector and the couple stress vector, respectively. Here the direct (index-free) notation in the sense of [15] is used. From (3.1) we obtain the local form of the balances of momentum and moment of momentum as well as the static boundary conditions. In the case of sufficiently smooth fields, the local equilibrium equations can be stated as follows

$$\nabla_s \cdot \mathbf{T} + \mathbf{q} = \mathbf{0}, \quad \nabla_s \cdot \mathbf{M} + \mathbf{T} \times + \mathbf{c} = \mathbf{0}. \quad (3.2)$$

Here the surface (plane) nabla operator  $\nabla_s$  is given as  $\nabla_s = \mathbf{i}_\alpha (\partial / \partial x_\alpha)$  with the Cartesian coordinates  $x_\alpha$ , and  $\mathbf{i}_\alpha$  being the unit base vectors. The Greek indices take the values 1 and 2. The tensors  $\mathbf{T}$  and  $\mathbf{M}$  denote the surface stress and couple stress tensors, respectively. They relate to  $\mathbf{t}_s$  and  $\mathbf{m}_s$  by the equations  $\boldsymbol{\nu} \cdot \mathbf{T} = \mathbf{t}_s$  and  $\boldsymbol{\nu} \cdot \mathbf{M} = \mathbf{m}_s$ , where  $\boldsymbol{\nu}$  is the outward normal vector to  $\mathcal{C}$ .  $\mathbf{T}$  and  $\mathbf{M}$  take the form

$$\mathbf{T} = T_{\alpha\beta} \mathbf{i}_\alpha \mathbf{i}_\beta + T_{\alpha 3} \mathbf{i}_\alpha \mathbf{n}, \quad \mathbf{M} = M_{\alpha\beta} \mathbf{i}_\alpha \mathbf{i}_\beta + M_{\alpha 3} \mathbf{i}_\alpha \mathbf{n} \quad (\alpha, \beta = 1, 2). \quad (3.3)$$

Let us introduce the linear strain measures

$$\mathbf{e} = \nabla_s \mathbf{v} + \mathbf{A} \times \boldsymbol{\theta}, \quad \mathbf{k} = \nabla_s \boldsymbol{\theta}, \quad (3.4)$$

where  $\mathbf{A} \equiv \mathbf{I} - \mathbf{n} \otimes \mathbf{n}$  is the first metric tensor, and  $\mathbf{n}$  the unit normal to  $\mathcal{M}$ . Applying the methodology presented in [4, 14], one can show that the linear strain measures are work-conjugated to the stress measures  $\mathbf{T}$  and  $\mathbf{M}$ .

For the isotropic plate, the surface strain energy  $W$  can be introduced by [4, 6, 8]

$$\begin{aligned} 2W = & \alpha_1 \text{tr}^2 \mathbf{e}_S + \alpha_2 \text{tr} \mathbf{e}_S^2 + \alpha_3 \text{tr} (\mathbf{e}_S \cdot \mathbf{e}_S^T) + \alpha_4 \mathbf{n} \cdot \mathbf{e}^T \cdot \mathbf{e} \cdot \mathbf{n} \\ & + \beta_1 \text{tr}^2 \mathbf{k}_S + \beta_2 \text{tr} \mathbf{k}_S^2 + \beta_3 \text{tr} (\mathbf{k}_S \cdot \mathbf{k}_S^T) + \beta_4 \mathbf{n} \cdot \mathbf{k}^T \cdot \mathbf{k} \cdot \mathbf{n}. \end{aligned} \quad (3.5)$$

Here  $\mathbf{e}_S = \mathbf{e} \cdot \mathbf{A}$ ,  $\mathbf{k}_S = \mathbf{k} \cdot \mathbf{A}$ , and  $\alpha_i, \beta_i$  are the elastic stiffness parameters,  $i = 1, 2, 3, 4$ . The constitutive equations are  $\mathbf{T} \equiv \partial W / \partial \mathbf{e}$  and  $\mathbf{M} \equiv \partial W / \partial \mathbf{k}$ .

The surface strain energy  $W$  must be positive definite, from which it follows [7]

$$\begin{aligned} 2\alpha_1 + \alpha_2 + \alpha_3 > 0, & \quad \alpha_2 + \alpha_3 > 0, & \quad \alpha_3 - \alpha_2 > 0, & \quad \alpha_4 > 0, \\ 2\beta_1 + \beta_2 + \beta_3 > 0, & \quad \beta_2 + \beta_3 > 0, & \quad \beta_3 - \beta_2 > 0, & \quad \beta_4 > 0. \end{aligned} \quad (3.6)$$

Note that for an isotropic three-dimensional micropolar solid we have only 6 elastic moduli, while the micropolar plate theory contains 8 elastic stiffness parameters. The increase in the number of parameters can be explained by at least two reasons:

- *Reduced symmetry of the constitutive equations.*  
In the case of two-dimensional equations, a smaller number of symmetry groups in comparison with the three-dimensional theory can be established. This fact is well-known also for other plate theories, see, e.g., [2, 6].
- *Reduction of three-dimensional equations to two-dimensional.*  
In the isotropic elasticity, material behavior is presented by two material parameters (e.g., Lamé's moduli). The number in the full Kirchhoff plate theory including both the in-plane and out-of-plane behavior is greater. Similar conclusions can be given for other plate theories, too.

### 3.3 Reduction of the Three-Dimensional Micropolar Elasticity Equations by the Through-the-Thickness Integration

Let us introduce the balance equations of the micropolar elasticity [10]. The equilibrium conditions of any part of a micropolar body occupying the volume  $V_* \subset V$  consist of the following relations

$$\begin{aligned} \mathbf{F}^* &\equiv \int_{V_*} \rho \mathbf{f} \, dV + \int_{S_*} \mathbf{t} \, dA = \mathbf{0}, \\ \mathbf{M}^* &\equiv \int_{V_*} \rho (\mathbf{r} \times \mathbf{f} + \mathbf{l}) \, dV + \int_{S_*} (\mathbf{r} \times \mathbf{t} + \mathbf{m}) \, dA = \mathbf{0}, \end{aligned} \quad (3.7)$$

where  $\mathbf{f}$  and  $\mathbf{l}$  are the mass forces and mass couples vectors, respectively,  $\rho$  is the density,  $\mathbf{r}$  is the position vector,  $S_* = \partial V_*$ ,  $\mathbf{t}$  and  $\mathbf{m}$  are the stress and couple stress vectors, respectively.  $\mathbf{F}^*$  and  $\mathbf{M}^*$  are the total force and the total couple acting on  $V_*$ , respectively. Hence, for any part of the micropolar body, (3.7)<sub>1</sub> states that the vector of total force is zero, while (3.7)<sub>2</sub> states that the vector of total moment is zero. With the relations  $\mathbf{n} \cdot \boldsymbol{\sigma} = \mathbf{t}$ ,  $\mathbf{n} \cdot \boldsymbol{\mu} = \mathbf{m}$ , the local equilibrium equations are

$$\nabla \cdot \boldsymbol{\sigma} + \rho \mathbf{f} = \mathbf{0}, \quad \nabla \cdot \boldsymbol{\mu} + \boldsymbol{\sigma}_\times + \rho \mathbf{l} = \mathbf{0}. \quad (3.8)$$

Now the nabla operator  $\nabla$  is a three-dimensional operator,  $\rho$  is the density, and  $\boldsymbol{\sigma}$  and  $\boldsymbol{\mu}$  are the stress and couple stress tensors, respectively.  $\boldsymbol{\sigma}_\times$  is the vectorial invariant of a second-order tensor  $\boldsymbol{\sigma}$ .

The small strains of the micropolar continuum are usually presented by the displacement vector  $\mathbf{u}$  and the vector of microrotation  $\boldsymbol{\vartheta}$ . The linear strain measures, i.e., the stretch tensor  $\mathbf{E}$  and the wryness tensor  $\mathbf{K}$ , are given by the relations

$$\mathbf{E} = \nabla \mathbf{u} + \boldsymbol{\vartheta} \times \mathbf{l}, \quad \mathbf{K} = \nabla \boldsymbol{\vartheta}. \quad (3.9)$$

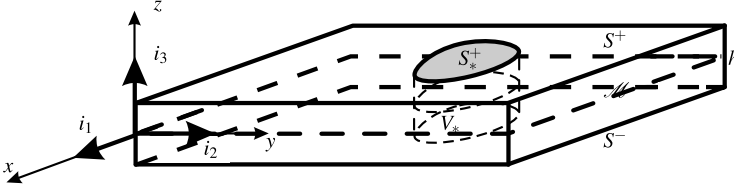


**Fig. 3.2** Plate-like body

The classical isotropic elasticity can be deduced by setting  $\kappa = \alpha = \beta = \gamma = 0$ . In this case, the stress tensor  $\boldsymbol{\sigma}$  will be a symmetric tensor. In addition,  $\boldsymbol{\mu}$  and  $\mathbf{l}$  vanish.

Finally, the isotropic elastic constitutive equations are

$$\boldsymbol{\sigma} = \lambda \text{tr} \mathbf{E} + \mu \mathbf{E}^T + (\mu + \kappa) \mathbf{K}, \quad \boldsymbol{\mu} = \alpha \text{tr} \mathbf{K} + \beta \mathbf{K}^T + \gamma \mathbf{K}. \quad (3.10)$$

The integration procedure is performed as follows. Let us assume that our plate-like body occupies a volume with one dimension which is significantly smaller in comparison with the other two. The coordinate  $z$  denotes this special direction and  $h$  is the plate thickness;  $z$  takes the values  $-h/2 \leq z \leq h/2$  (Fig. 3.2). The boundary conditions of the upper (+) and lower (-) plate surfaces can be given by

$$\mathbf{n}^\pm \cdot \boldsymbol{\sigma} = \mathbf{t}^\pm, \quad \mathbf{n}^\pm \cdot \boldsymbol{\mu} = \mathbf{m}^\pm, \quad (3.11)$$

where  $\mathbf{t}^\pm$  and  $\mathbf{m}^\pm$  are the surface loads (forces and moments) and  $\mathbf{n}^\pm = \mathbf{i}_3$ .

The main idea of the reduction procedure is the application of the 3D equilibrium conditions (3.7) to any volume  $V_*$  of the plate-like body and the transformation of the results to the 2D case as in (3.1). Following [1], we transform (3.7) into the relations

$$\begin{aligned} \mathbf{F}^* &= \int_{\mathcal{M}_*} \mathbf{q} \, dA + \int_{\mathcal{C}_*} \boldsymbol{\nu} \cdot \langle \boldsymbol{\sigma} \rangle \, ds = \mathbf{0}, & \langle (\dots) \rangle &= \int_{-h/2}^{h/2} (\dots) \, dz, \\ \mathbf{M}^* &= \int_{\mathcal{M}_*} [\mathbf{x} \times \mathbf{q} + \mathbf{c}] \, dA \\ &+ \int_{\mathcal{C}_*} [\boldsymbol{\nu} \cdot \langle \boldsymbol{\mu} \rangle - \boldsymbol{\nu} \cdot \langle z \boldsymbol{\sigma} \times \mathbf{i}_3 \rangle - \boldsymbol{\nu} \cdot \langle \boldsymbol{\sigma} \rangle \times \mathbf{x}] \, dA = \mathbf{0}, \end{aligned} \quad (3.12)$$

where the following notations are introduced

$$\begin{aligned} \mathbf{q} &= \langle \rho \mathbf{f} \rangle + \mathbf{t}^+ + \mathbf{t}^-, \\ \mathbf{c} &= \langle \rho \mathbf{l} \rangle + \mathbf{m}^+ + \mathbf{m}^- + \mathbf{i}_3 \times \langle \rho z \mathbf{f} \rangle + \frac{h}{2} \mathbf{i}_3 \times (\mathbf{t}^+ - \mathbf{t}^-). \end{aligned}$$

The comparison of (3.12) and (3.1) leads to the determination of the stress resultant and stress couple tensors by the following relations

$$\mathbf{T} = \langle \mathbf{A} \cdot \boldsymbol{\sigma} \rangle, \quad \mathbf{M} = \langle \mathbf{A} \cdot \boldsymbol{\mu} \rangle - \langle \mathbf{A} \cdot z\boldsymbol{\sigma} \times \mathbf{i}_3 \rangle. \quad (3.13)$$

From the second equation in (3.13), it follows that the components  $M_{\alpha 3}$  depend only on the couple stress tensor  $\boldsymbol{\mu}$ . Indeed,  $\mathbf{M} \cdot \mathbf{i}_3 = \langle \mathbf{A} \cdot \boldsymbol{\mu} \cdot \mathbf{i}_3 \rangle$ .

To establish the relations with the vectors  $\mathbf{u}$  and  $\boldsymbol{\vartheta}$  used in the 3D theory and their analogues  $\mathbf{v}$  and  $\boldsymbol{\theta}$  in the 2D theory, we use the following approximation of  $\mathbf{u}$  and  $\boldsymbol{\vartheta}$ , see [1] for details,

$$\begin{aligned} \mathbf{u}(x, y, z) &= \mathbf{v}(x, y) - z\boldsymbol{\phi}(x, y), \\ \boldsymbol{\vartheta} &= \boldsymbol{\phi}(x, y) \times \mathbf{i}_3 + \vartheta_3(x, y)\mathbf{i}_3 = \boldsymbol{\theta}, \quad \boldsymbol{\phi} \cdot \mathbf{i}_3 = 0. \end{aligned} \quad (3.14)$$

This means that the couple stress tensor  $\boldsymbol{\mu}$  does not depend on  $z$ , while the stress tensor  $\boldsymbol{\sigma}$  depends on  $z$  linearly as in [10]. But the approximation (3.14) is more restrictive than the one applied by Eringen [10]. As a result, the effective stiffness parameters can be estimated as

$$\begin{aligned} \alpha_1 &= \tilde{\lambda}h, \quad \tilde{\lambda} \equiv \frac{\lambda(2\mu + \kappa)}{\lambda + 2\mu + \kappa}, \\ \alpha_2 &= \mu h, \quad \alpha_3 = (\mu + \kappa)h, \quad \alpha_4 = (\mu + \kappa)h, \\ \beta_1 &= \alpha h - \mu \frac{h^3}{12}, \quad \beta_2 = \beta h - \tilde{\lambda} \frac{h^3}{12}, \\ \beta_3 &= \gamma h + (2\mu + \kappa + \tilde{\lambda}) \frac{h^3}{12}, \quad \beta_4 = \gamma h. \end{aligned}$$

The in-plane stiffness parameters  $\alpha_1, \alpha_3, \alpha_3$ , and the transverse shear stiffness  $\alpha_4$  depend linearly on  $h$ . The dependence of  $\beta_i, i = 1, \dots, 4$ , on  $h$  is more complicated. The parameters  $\beta_i$  have linear asymptotes when  $h$  tends to zero, i.e.,  $\beta_i \sim h$ . The considered case differs from the cases of Kirchhoff's and Reissner's plates when  $\beta_i \sim h^3$ .

Introducing the engineering constants

$$G = \frac{2\mu + \kappa}{2}, \quad \nu = \frac{\lambda}{2\lambda + 2\mu + \kappa}, \quad l_b^2 = \frac{\gamma}{2(2\mu + \kappa)},$$

where  $G$  is the shear modulus,  $\nu$  the Poisson ratio,  $l_b$  the characteristic length under bending, see [10], we obtain the expression

$$D = \frac{Gh^3}{12(1 - \nu)} \left[ 1 + 2 \frac{l_b^2}{h^2} \right]. \quad (3.15)$$

The dependence  $D/\tilde{D}$  on  $h$  is given in Fig. 3.3, where  $\tilde{D} = Gh^3/[12(1 - \nu)]$  is the value of the bending stiffness used by Eringen [10]. From Fig. 3.3 it can be seen that the micropolar properties are inessential if  $h > 2l_b$ . The values of the elastic stiffness parameters for two porous materials are given in Table 3.1. Here we have used the experimental data presented by Lakes [12, 13]. The index \* denotes

the case of the material without the micropolar properties, i.e., if  $\kappa = \alpha = \beta = \gamma = 0$ .

To calculate the elastic stiffness we have used the approximation (3.14). Let us note that in the literature on the shell theory there are many different approaches to derive the shell equations from the 3D elasticity which lead to different values of the stiffness parameters, see [4, 14] among others. For the Cosserat continuum the derivation of the shell theories are given in many publications, see the reviews in [1, 3] and [19]. This means that the elastic stiffness parameters presented above can be considered as some estimates. In other words, these parameters show the influence of the micropolar properties. In particular, (3.15) demonstrates the size-effect which is well-known in the micropolar elasticity, see [10, 12, 13]. The analysis of (3.15) shows that the influence of the micropolar properties is essential if the thickness of the plate  $h$  has the same value as the characteristic length of the microstructure of the material.

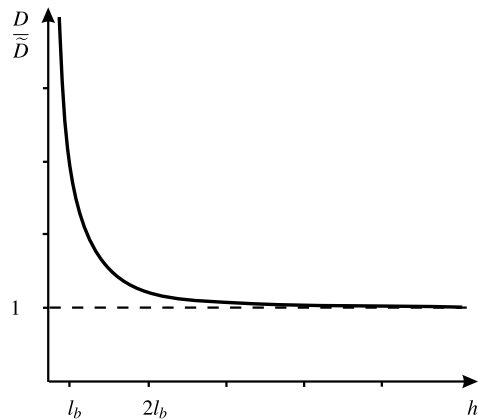


**Fig. 3.3** Dimensionless bending stiffness  $D/\bar{D}$  vs. the dimensionless thickness  $h/l_b$

**Table 3.1** Effective stiffness of a plate made of different foams ( $h$  has dimension  $m$ )

Elastic constants	Foam, PU	Foam, PU *	Foam, PS	Foam, PS *
$\alpha_1, N/m 10^6$	$0.165h$	$0.165h$	$138.67h$	$138.67h$
$\alpha_2, N/m 10^6$	$1.001h$	$1.1h$	$99.84h$	$104h$
$\alpha_3, N/m 10^6$	$1.199h$	$1.1h$	$108.16h$	$104h$
$\alpha_4, N/m 10^6$	$1.199h$	$1.1h$	$108.16h$	$104h$
$\beta_1, N\cdot m 10^6$	$-2.6 \times 10^{-6}h - 0.083h^3$	$-0.092h^3$	$-6.7 \times 10^{-6}h - 8.3h^3$	$-8.67h^3$
$\beta_2, N\cdot m 10^6$	$-10^{-4}h - 0.014h^3$	$-0.014h^3$	$-2.5 \times 10^{-5}h + 11.6h^3$	$-11.5h^3$
$\beta_3, N\cdot m 10^6$	$1.1 \times 10^{-4}h + 0.197h^3$	$0.197h^3$	$4.5 \times 10^{-5}h + 28.9h^3$	$28.8h^3$
$\beta_4, N\cdot m 10^6$	$1.1 \times 10^{-4}h$	0	$4.5 \times 10^{-5}h$	0

### 3.4 Conclusion

In this paper, we present the general six-parametric or micropolar linear plate linear theory with two vector fields of the translations and rotations as the independent kinematic variables. Within the proposed theory one may take into account an external surface drilling moment. We discuss the relations between the direct approach and the through-the-thickness integration procedure to derive the plate equilibrium equations and the constitutive equations. The influence of the micropolar properties on the stiffness parameters of the plate is illustrated for two foams.

**Acknowledgements** The second author was supported by the RFBR with the grant No. 09-01-00459 and by the DFG with the grant No. AL 341/31-1.

### References

1. Altenbach, H., Eremeyev, V.A.: On the linear theory of micropolar plates. *Z. Angew. Math. Mech.* **4**(89), 242–256 (2009)
2. Altenbach, H., Zhilin, P.A.: A general theory of elastic simple shells. *Usp. Mekh.* **11**(4) (1988). In Russian
3. Altenbach, J., Altenbach, H., Eremeyev, V.A.: On generalized Cosserat-type theories of plates and shells. A short review and bibliography. *Arch. Appl. Mech.* **80**, 73–92 (2010)
4. Chróścielewski, J., Makowski, J., Pietraszkiewicz, W.: *Statyka i dynamika powłok wielopłatowych. Nieliniowa teoria i metoda elementów skończonych*. Wydawnictwo IPPT PAN, Warszawa (2004)
5. Cosserat, E., Cosserat, F.: *Théorie des corps déformables*. Herman et Fils, Paris (1909)
6. Eremeyev, V.A., Pietraszkiewicz, W.: Local symmetry group in the general theory of elastic shells. *J. Elast.* **85**(2), 125–152 (2006)
7. Eremeyev, V.A., Zubov, L.M.: On constitutive inequalities in nonlinear theory of elastic shells. *Z. Angew. Math. Mech.* **87**(2), 94–101 (2007)
8. Eremeyev, V.A., Zubov, L.M.: *Mechanics of Elastic Shells*. Nauka, Moscow (2008). In Russian
9. Ericksen, J.L., Truesdell, C.: Exact theory of stress and strain in rods and shells. *Arch. Ration. Mech. Anal.* **1**(1), 295–323 (1958)
10. Eringen, A.C.: *Microcontinuum Field Theory. I. Foundations and Solids*. Springer, New York (1999)
11. Kröner, E. (ed.): *Mechanics of Generalized Continua. Proceedings of the IUTAM-Symposium on the Generalized Cosserat Continuum and the Continuum Theory of Dislocations with Applications*, Freudenstadt and Stuttgart (Germany), 1967, vol. 16. Springer, Berlin (1968)
12. Lakes, R.S.: Experimental microelasticity of two porous solids. *Int. J. Solids Struct.* **22**, 55–63 (1986)
13. Lakes, R.S.: Experimental micro mechanics methods for conventional and negative Poisson's ratio cellular solids as Cosserat continua. *Trans. ASME. J. Eng. Mat. Technol.* **113**, 148–155 (1991)
14. Libai, A., Simmonds, J.G.: *The Nonlinear Theory of Elastic Shells*, 2nd edn. Cambridge University Press, Cambridge (1998)
15. Lurie, A.I.: *Theory of Elasticity. Foundations of Engineering Mechanics*. Springer, Berlin (2005)



16. Naghdi, P.: The theory of plates and shells. In: Flügge, S. (ed.) *Handbuch der Physik*, vol. VIa/2, pp. 425–640. Springer, Heidelberg (1972)
17. Rubin, M.B.: *Cosserat Theories: Shells, Rods and Points*. Kluwer, Dordrecht (2000)
18. Truesdell, C.: Die Entwicklung des Drallsatzes. *Z. Angew. Math. Mech.* **44**(4/5), 149–158 (1964)
19. Zubov, L.M.: Micropolar-shell equilibrium equations. *Dokl. Phys.* **54**(6), 290–293 (2009)